Atmos. Meas. Tech., 9, 5315–5329, 2016
www.atmos-meas-tech.net/9/5315/2016/
doi:10.5194/amt-9-5315-2016

Atmospheric Measurement Techniques
Open Access
EGU

Sensitive detection of *n*-alkanes using a mixed ionization mode proton-transfer-reaction mass spectrometer

Omar Amador-Muñoz[1,2], Pawel K. Misztal[1], Robin Weber[1], David R. Worton[3], Haofei Zhang[1], Greg Drozd[1], and Allen H. Goldstein[1]

[1]Department of Environmental Science, Policy, and Management, University of California, Berkeley, CA, USA
[2]Centro de Ciencias de la Atmosfera, Universidad Nacional Autonoma de Mexico, Mexico
[3]National Physical Laboratory, Teddington, Middlesex, TW11 0LW, UK

Correspondence to: Omar Amador-Muñoz (oam@atmosfera.unam.mx)

Received: 2 March 2016 – Published in Atmos. Meas. Tech. Discuss.: 15 April 2016
Revised: 10 October 2016 – Accepted: 17 October 2016 – Published: 7 November 2016

Abstract. Proton-transfer-reaction mass spectrometry (PTR-MS) is a technique that is widely used to detect volatile organic compounds (VOCs) with proton affinities higher than water. However, *n*-alkanes generally have a lower proton affinity than water and therefore proton transfer (PT) by reaction with H_3O^+ is not an effective mechanism for their detection. In this study, we developed a method using a conventional PTR-MS to detect *n*-alkanes by optimizing ion source and drift tube conditions to vary the relative amounts of different primary ions (H_3O^+, O_2^+, NO^+) in the reaction chamber (drift tube). There are very few studies on O_2^+ detection of alkanes and the mixed mode has never been proposed before. We determined the optimum conditions and the resulting reaction mechanisms, allowing detection of *n*-alkanes from *n*-pentane to *n*-tridecane. These compounds are mostly emitted by evaporative/combustion process from fossil fuel use. The charge transfer (CT) mechanism observed with O_2^+ was the main reaction channel for *n*-heptane and longer *n*-alkanes, while for *n*-pentane and *n*-hexane the main reaction channel was hydride abstraction (HA). Maximum sensitivities were obtained at low E/N ratios (83 Td), low water flow (2 sccm) and high O_2^+ / NO^+ ratios ($U_{so} = 180$ V). Isotopic ^{13}C contribution was taken into account by subtracting fractions of the preceding ^{12}C ion signal based on the number of carbon atoms and the natural abundance of ^{13}C (i.e., 5.6 % for *n*-pentane and 14.5 % for *n*-tridecane). After accounting for isotopic distributions, we found that PT cannot be observed for *n*-alkanes smaller than *n*-decane. Instead, protonated water clusters of *n*-alkanes ($M \cdot H_3O^+$) species were observed with higher abundance using lower O_2^+ and higher water cluster fractions. $M \cdot H_3O^+$ species are probably the source for the $M + H^+$ species observed from *n*-decane to *n*-tridecane. Normalized sensitivities to O_2^+ or to the sum of $O_2^+ + NO^+$ were determined to be a good metric with which to compare sensitivities for *n*-alkane detection between experiments. Double hydride abstraction was observed from the reaction with O_2^+. Sensitivity to CT increased with carbon chain length from *n*-pentane to *n*-dodecane, sensitivity to HA increased from *n*-heptane to *n*-dodecane and sensitivity to PT increased from *n*-decane to *n*-tridecane. Sensitivity to CT exponentially decreased with molecular ionization energy, which is inversely related to the carbon chain length. We introduce a calibrated fragmentation algorithm as a method to determine the concentrations of *n*-alkanes and demonstrate its effectiveness using a custom *n*-alkane mixture and a much more complex oil example representing perhaps the most difficult mixture available for application of the method. We define optimum conditions for using the mixed ionization mode to measure *n*-alkanes in conventional PTR-MS instruments regardless of whether they are equipped with switchable reagent ion (SRI) capabilities.

1 Introduction

Proton-transfer-reaction mass spectrometry (PTR-MS) has been extensively used to measure volatile organic compounds (VOCs) (e.g., de Gouw and Warneke, 2007). PTR-MS is normally optimized for just H_3O^+ ionization but that does not allow efficient detection of *n*-alkanes and some

other species that are extremely important for air quality, atmospheric chemistry and source emission characterization. This technique offers close to real-time data acquisition and low detection limits (low pptv) (Karl et al., 2012). Chemical ionization (CI) from different reagent ions is also now possible in PTR-MS instruments equipped with switchable reagent ions (SRI) and with selected-ion flow tube mass spectrometers (SIFT-MS). CI is achieved mainly through reaction with an atomic or molecular ion following four possible reaction processes: charge transfer (CT), proton transfer (PT), hydride abstraction (HA) or adduct formation (Ellis and Mayhew, 2014). The reactions of H_3O^+ with VOCs (Reaction R1) are thermodynamically favored when the proton affinity of its conjugate base, H_2O, is lower ($691 \pm 3\,\mathrm{kJ\,mol^{-1}}$) than that of the VOCs in question (Hunter and Lias, 1998). However, the proton affinities for commonly encountered inorganic compounds in air, such as nitrogen and oxygen, and also for some haloalkanes and alkanes, are higher and therefore they are not detectable by PT (Reaction R1).

$$\mathrm{H_3O^+ + C_nH_{2n+2}}\,\big|\,\mathrm{n \geq 10 \rightarrow C_nH_{2n+2} + H^+ + H_2O}$$
Proton transfer (R1)

Alkanes are among the most abundant compounds in urban air (Amador-Muñoz et al., 2011). Biogenic sources may also emit n-alkanes and several studies have demonstrated that VOCs exhaled from the lungs (King et al., 2010) contain n-alkanes. Petroleum-derived air pollution sources, including gasoline and diesel fuels (Gentner et al., 2012, 2013), motor oils (Worton et al., 2014) or crude oil (Drozd et al., 2015; Worton et al., 2015), contain significant amounts of alkanes. These compounds react in the atmosphere to produce ozone and secondary organic aerosol (Jordan et al., 2008; Lim and Ziemann, 2005) with implications for climate and human health. Adapting PTR-MS to measure alkanes simultaneously along with other VOCs is therefore of significant interest. Previous studies have been conducted to explore measurement of n-alkanes in PTR-MS experiments (Erickson et al., 2014; Jobson et al., 2005) in conventional H_3O^+ mode. However, proton transfer reaction products are mostly unobserved for alkanes because the proton affinity of most alkanes is lower than that of water and in the case of longer alkanes ($C \geq 10$) it is only very slightly higher than water potentially leading to backward reactions. Instead, association is the predominant reaction mechanism observed at room temperature for n-alkanes (Arnold et al., 1998; Španěl and Smith, 1998).

n-Alkanes ($N_c = 2$–12) can react with NO^+ typically through hydride abstraction (Arnold et al., 1997, 1998; Inomata et al., 2013; Lias et al., 1976; Searles and Sieck, 1970, Španěl and Smith, 1998; Wilson et al., 2003) (Reaction R2).

$$\mathrm{NO^+ + C_nH_{2n+2} \rightarrow C_nH^+_{2n+1} + (NO + H)}$$
Hydride abstraction (R2)

Reactions with O_2^+ have been observed to proceed by charge transfer (Reaction R3) ($N_c = 2$–12) (Arnold et al., 1997; Francis et al., 2007; Španěl and Smith, 1998; Wilson et al., 2003), hydride abstraction (Reaction R4) ($N_c = 2$–4) (Francis et al., 2007; Wilson et al., 2003) and double hydride abstraction (DHA) (Reaction R5) ($N_c = 2$–3) (Francis et al., 2007; Wilson et al., 2003).

$$\mathrm{O_2^+ + C_nH_{2n+2} \rightarrow C_nH^+_{2n+2} + O_2}$$
Charge transfer (R3)

$$\mathrm{O_2^+ + C_nH_{2n+2} \rightarrow C_nH^+_{2n+1} + (O_2 + H)}$$
Hydride abstraction (R4)

$$\mathrm{O_2^+ + C_nH_{2n+2} \rightarrow C_nH^+_{2n} + (O_2 + 2H)}$$
Double hydride abstraction (R5)

However, reactions with O_2 are often dissociative because the ionization energy (IE) of O_2 (12.07 eV; NIST Chemistry Web Book, Linstrom and Mallard, 2005) is higher than the vast majority of organic molecules, leading to significant fragmentation (Blake et al., 2006; Wyche et al., 2005). For this reason, application of O_2^+ ionization has so far been limited in the PTR-MS community. It is possible to suppress fragmentation by keeping the field strength (E/N, where E is the electric field strength and N the buffer gas density) in the drift tube sufficiently low. Typical PTR-MS conditions have O_2^+ impurities typically ranging from 1 to 5 % of H_3O^+ (de Gouw and Warneke, 2007). Recently, the PTR-MS instrument has been equipped with an SRI capability, which allows for switching between more pure H_3O^+, NO^+ and O_2^+ ion modes (Jordan et al., 2009; Knighton et al., 2009; Karl et al., 2012; Inomata et al., 2013; Koss et al., 2016).

In this study we show how a PTR-MS (without SRI capability) can successfully be optimized to measure n-alkanes and other major VOCs at the same time by making O_2^+, H_3O^+ and NO^+ reagent ions simultaneously available. We also define the reaction mechanisms leading to detection of n-alkanes using these three reactant ions.

2 Methods

2.1 Proton-transfer-reaction mass spectrometer

PTR-MS is a highly sensitive technique for quantification of atmospheric VOCs close to real time (10 Hz) (Karl et al., 2002). The operation and fundamental principles of PTR-MS have been described in detail previously (Hansel et al., 1995; Lindinger et al., 1998; de Gouw et al., 2003; Holzinger et al., 2005), and therefore only a brief description is given here. The three main components of the PTR-MS are the ion source, drift tube and detector. In conventional PTR-MS, the

Table 1. n-Alkanes used in experiments: formula, molecular weight (MW), monitored ions indicating hydride abstraction (HA), charge transfer (CT) and proton transfer (PT), isotopic contribution ($^{13}C/^{12}C$), ionization energies (IE) and proton affinities (PA). Water proton affinity: 166.5 ± 2 kcal mol^{-1} (Lias et al., 1984).

No.	Compound	Formula	MW,	Mechanism and ions monitored			$^{13}C/^{12}C$	IE,	PA[c]
			Da	HA, m/z	CT, m/z	PT, m/z	%	eV	Kcal/mol
1	n-pentane	C_5H_{12}	72	71	72	73	5.6	10.28[a]	–
2	n-hexane	C_6H_{14}	86	85	86	87	6.7	10.13[a]	160.7
3	n-heptane	C_7H_{16}	100	99	100	101	7.8	9.93[a]	–
4	n-octane	C_8H_{18}	114	113	114	115	8.9	9.80[a]	163.4
5	n-nonane	C_9H_{20}	128	127	128	129	10.0	9.71[a]	–
6	n-decane	$C_{10}H_{22}$	142	141	142	143	11.1	9.65[a]	165.0
7	n-undecane	$C_{11}H_{24}$	156	155	156	157	12.2	9.56[a]	–
8	n-dodecane	$C_{12}H_{26}$	170	169	170	171	13.3	9.48[b]	165.6
9	n-tridecane	$C_{13}H_{28}$	184	183	184	185	14.5	9.42[b]	–

[a] NIST chemistry web book (http://webbook.nist.gov). [b] Zhou et al. (2010); theoretical values calculated by density functional theory at B3P86/6-31++G(d,p) level. [c] Hunter and East (2002).

ion source is a hollow cathode that produces hydronium ion (H_3O^+), using a plasma discharge and water (H_2O). During this process, some O_2^+ and NO^+ ions are also produced. The extracted ions from the ion source are accelerated in the drift tube by an electrical field (E). The air containing VOCs to be analyzed operates as buffer gas number density (N) and is also introduced into the drift tube. Reagent ions and VOCs selectively collide under specific E/N ratios, maintaining a buffer gas pressure of typically 2–2.3 mbar. The proton transfer and any other reactions occur in the drift tube and their product ions are filtered by a quadrupole mass spectrometer and counted by a secondary electron multiplier (SEM).

Different reactions in the drift tube can be favored according to the abundance and ratios among the ions generated in the ion source. The PTR-MS ion source is typically optimized so that H_3O^+ is the most abundant ion. However, water can be substituted by pure O_2 or a mixture of O_2 and N_2 to produce O_2^+ or NO^+ as the dominant ions, respectively, as is the case in instruments equipped with SRI (Inomata et al., 2013; Jordan et al., 2009; Karl et al., 2012). In a conventional PTR-MS the relative abundance of O_2^+ and NO^+ ions can be enhanced compared to H_3O^+ by increasing the source out voltage (U_{SO}).

We optimized ion source and drift tube conditions to vary the relative amounts of ions produced using a conventional PTR-MS to determine the best conditions for detecting n-alkanes with different carbon chain lengths. Drift tube temperature and drift tube pressure were kept constant at 60 °C and at 2.00 ± 0.02 mbar, respectively. Mass scans were recorded from 20 to 220 Da (200 ms dwell time) for 45 cycles in each experiment. This range included the H_3O^+ isotopic primary ion (m/z 21), NO^+ ion (m/z 30), isotopic O_2^+ ion (m/z 34) and water clusters (mono-hydrated, m/z 37, and bi-hydrated, m/z 55). O_2^+ count rates were calculated from the isotopic oxygen signal at m/z 34, times 250; H_3O^+ counts were calculated from the isotopic contribution at m/z 21, times 500. Optimization tests included adjusting the amount of water supplied to the ion source, adjusting the drift tube voltage and adjusting the source out voltage. Water flow to the ion source to generate H_3O^+ was tested at two conditions: low water flow (LWF) at 2 sccm and high water flow (HWF) at 6 sccm. The field strength of the drift tube, E/N, was tested under five sets of conditions including 83, 91, 101, 109 and 122 Td (1 Td $= 10^{-17}$ V cm^2 molecule^{-1}), which were achieved by setting the drift tube (U_{drift}) voltage to 343, 375, 419, 461 and 505 V, respectively. To vary all primary ions in the hollow cathode discharge ion source, the source out voltage (U_{SO}) was cycled between 60, 90, 120, 150 and 180 V.

2.2 Experimental setup and methods

All measurements reported here were done using a PTR-MS with a quadrupole mass spectrometer (Ionicon Analytik). Pure standards of nine n-alkanes ranging from n-pentane to n-tridecane were used: n-pentane (≥ 99 %), n-hexane (≥ 99 %), n-decane (≥ 99 %) and n-undecane (≥ 99 %) were purchased from Sigma-Aldrich; n-heptane (99 %) from Spectrum; n-octane (> 99 %) and n-tridecane (> 99 %) from Acros Organics; and n-nonane (99 %) and n-dodecane (> 99 %) from Alfa Aesar. Water used for producing H_3O^+ ions was obtained from BDH Reagents & Chemicals. Table 1 shows the molecular formula, molecular weight, ^{13}C isotopic abundance and IEs for these nine n-alkanes along with the corresponding ions for each reaction mechanism. These n-alkane standards were introduced into a custom-built flow tube system (Zhang et al., 2013) to mix and dilute the n-alkanes with zero air (Fig. 1). The standards in liquid form were injected with a syringe pump (Kd Scientific) at 0.2 µL min^{-1} into a zero air stream produced by a zero air generator (Aadco 737) and introduced

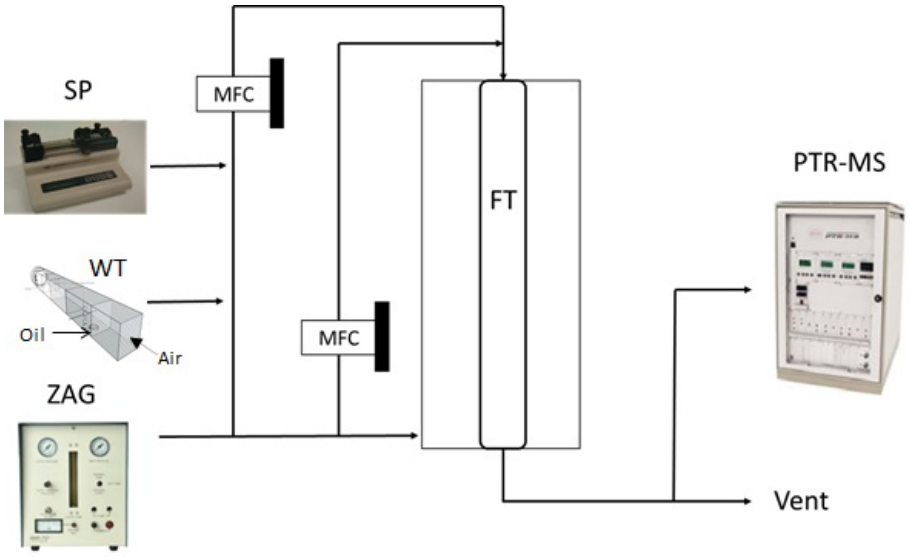

Figure 1. Schematic of the flow tube (FT) used to mix and dilute the n-alkanes coming from the syringe pump (SP) and wind tunnel (WT) with zero air produced by a generator (ZAG), followed by analysis using proton-transfer-reaction mass spectrometry (PTR-MS).

into the flow tube throughout a Silcosteel transfer line heated to $50 \pm 4\,^{\circ}\mathrm{C}$. A total flow of $2.3\,\mathrm{L\,min^{-1}}$ was maintained through the flow tube for the experiments. Four sets of experiments were conducted: a first set of experiments to determine reaction mechanisms and optimize conditions for reaction with different ions, a second set of experiments to determine sensitivities for individual n-alkanes under optimized conditions, a third set of experiments to test an algorithm to estimate the n-alkanes concentrations in a standard mixture and a fourth set of experiments to test the algorithm to measure n-alkanes evaporated from an oil sample.

2.2.1 Optimization experiments

To determine the reaction mechanisms of n-alkanes in the PTR-MS and to optimize conditions for their detection, a constant flow of $40\,\mathrm{mL\,min^{-1}}$ (MKS flow controller) of n-hexane (1340 ppbv), n-decane (445 ppbv), n-nonane (482 ppbv), n-undecane (406 ppbv) and n-dodecane (377 ppbv) were introduced into the flow tube. The mechanism of reaction was determined from the observed m/z ratios. Proton transfer was indicated by the addition of 1 amu to the parent mass (M + H), charge transfer by detection of the parent mass (M), hydride abstraction by the loss of 1 amu (M − H) and double hydride extraction by the loss of 2 amu (M − 2H). Relative humidity (RH) was controlled at $< 2\,\%$. RH and room temperature were recorded every 30 s (Humitter 50Y, Vaisala). Sensitivities ($\mathrm{cps\,ppbv^{-1}}$) to charge transfer, hydride abstraction and proton transfer reactions were determined for all 50 different combinations of E/N ratios, primary ions abundances and water flow conditions. Sensitivities were corrected by subtracting the isotopic ^{13}C contribution of the preceding ^{12}C ion (Table 1).

2.2.2 Sensitivity determinations

To determine PTR-MS measurement sensitivities using optimized conditions under typical ambient humidity conditions, calibration curves were generated by introducing each individual n-alkane into the flow tube at three different flow rates (20, 50 and $80\,\mathrm{mL\,min^{-1}}$) while the total flow was maintained constant at $2.3\,\mathrm{L\,min^{-1}}$. These experiments were conducted at room temperature with an RH of 30 %. Sensitivities were corrected by subtracting the isotopic ^{13}C contribution of the preceding ^{12}C ion (Table 1). Table S1 shows the concentration ranges generated for each n-alkane.

2.3 Approach to quantifying n-alkanes mixtures

Fragmentation of n-alkanes due to O_2^+ ionization represents a challenge in the quantification of complex mixtures. We developed an approach which uses a calibrated fragmentation algorithm to take into account the contributions of overlapping fragments from larger n-alkanes to the masses where smaller n-alkanes are measured. The algorithm consists of two stages.

1. Algorithm calibration uses single pure n-alkanes from n-pentane to n-tridecane:

   a. Calculate the weighted cps to 1×10^6 of O_2^+ for an individual pure n-alkane, with O_2^+ quantified as the signal of m/z 34 times 250.

   $$\mathrm{wcps}\left(O_2^+\right) = \frac{\mathrm{cps(nAlk)}}{\mathrm{cps}(O_2^+)} \times 10^6 \quad (1)$$

   b. Calculate weighted sensitivities ($\mathrm{wS}(O_2^+)$) for individual pure n-alkanes from the slope of the

weighted signal of the parent ion and the introduced concentrations of the alkane.

$$\mathrm{wS}\left(\mathrm{O}_2^+\right) = \frac{\mathrm{wcps}\left(\mathrm{O}_2^+\right)}{\mathrm{ppbv}} \times 10^6 \quad (2)$$

c. Calculate the fragment contribution distribution (FCD) for each fragment relative to the molecular ion (mol ion) of each individual pure n-alkane.

$$\mathrm{FCD} = \frac{\mathrm{cps(fragment)}}{\mathrm{cps(mol\ ion)}} \quad (3)$$

2. Algorithm application measures unknown mixture of n-alkanes:

a. Calculate the excess signal of the larger n-alkanes on the target ion.

$$\text{Excess signal}_i = \sum_j^n [(\mathrm{wcps\_mol\_ion}\left(\mathrm{O}_2^+\right)_j \cdot \mathrm{FCD}_j)], \quad (4)$$

where

- i is the n-alkane target ion;
- $j = i + 1$, the carbon number of larger n-alkane in the mixture;
- n is the carbon number of the largest n-alkane in the mixture;
- $\mathrm{wcps\_mol\_ion}(\mathrm{O}_2^+)$ is the weighted signal from O_2^+ on the molecular ion;
- FCD_j is the fragment contribution distribution of the target ion on the molecular ion of the larger n-alkane.

b. Subtract the "excess signal" from the weighted signal from O_2^+ on the molecular ion of the target compound.

$$\text{Pure signal} = \mathrm{wcps\_mol\_ion}(\mathrm{O}_2^+) - \text{excess signal} \quad (5)$$

c. Estimate ppbv by dividing "pure signal" by "$\mathrm{wS}(\mathrm{O}_2^+)$" of the target compound.

The algorithm was applied to estimate individual n-alkanes contained in a mixture of nine n-alkanes at three concentration levels (Table S2).

2.4 Measuring n-alkanes in an oil sample

To test the algorithm on a real sample, we analyzed gas phase n-alkanes evaporated from an MC252 oil sample. Oil (100 mL) in a dish was placed into the wind tunnel (2.9 m × 0.305 m × 0.305 m) with filtered air flowing at 2 m s^{-1} for 27.5 h. The PTR-MS sampled from the wind tunnel downstream of the evaporating oil with a constant flow of 0.186 m^3 s^{-1}. The evaporated mass concentration of n-alkanes measured by PTR-MS was integrated over 2, 8 and 12 h evaporation time.

To compare the n-alkanes observed by PTR-MS evaporating into the gas phase estimated with the algorithm, we analyzed the fresh liquid oil MC252 and remaining liquid oil at 2, 8 and 12 h evaporation times, using two-dimensional gas chromatography with high-resolution time-of-flight mass spectrometry and vacuum UV ionization ($\mathrm{GC} \times \mathrm{GC}$ / VUV − HRTOFMS) (Isaacman et al., 2012). Analysis conditions and MC252 oil characteristics are detailed in the Supplement.

3 Results

3.1 Relative ion abundances used to determine n-alkane reaction mechanisms

The relative abundance of reactant ions varied as a function of E/N ratios, U_{SO} voltages and water flows. Under normal PTR-MS conditions optimized for $\mathrm{H_3O^+}$, there are still O_2^+ and $\mathrm{NO^+}$ ions produced as byproducts in the ion source discharge. In our experiments, conditions were adjusted to enhance the relative amounts of O_2^+ and $\mathrm{NO^+}$ by decreasing the water flow from 6 to 2 sccm and increasing the U_{SO} from 60 to 180 V (Figs. 2, S1). The optimal flow rate of 2 sccm was chosen based on the relatively highest O_2^+ / $\mathrm{H_3O^+}$ ratio as well as the total absolute O_2^+ ion abundance at non-saturating conditions. Depending on the type of the ion source in other instruments and the ion source cleanliness, the actual $\mathrm{H_2O}$ flow rates may result in different equilibria. O_2^+ percentage relative to $\mathrm{H_3O^+}$ in LWF ranged from 34 to 270 % (U_{SO} from 60 to 180 V) and in HWF from 5 to 68 %. $\mathrm{NO^+}$ relative to O_2^+ observed in LWF ranged from 6 and 21 % and in HWF from 1 to 4 %. O_2^+ count rates were on average around 10 times higher than $\mathrm{NO^+}$ count rates. With HWF and low E/N, excessive water clusters were observed, which led to a decline in primary ions.

3.2 Maximizing sensitivity and determining dominant reaction mechanisms

The dominant reaction mechanism occurring for different n-alkanes, and also the overall sensitivities of detection, varied as a function of the relative abundance of different primary ions and could be controlled by varying U_{SO}, water flow and E/N ratio. The absolute sensitivities varied substantially with U_{SO} for different n-alkanes, while low E/N ensured the highest sensitivity for all the n-alkanes. Maximum sensitivities from n-nonane to n-dodecane were obtained at LWF, the lowest E/N ratios (83 Td) and the maximum U_{SO} (180 V). Figure 2 shows the sensitivities (cps ppbv^{-1}) for two example n-alkanes: n-hexane and n-decane. Three ions were plot-

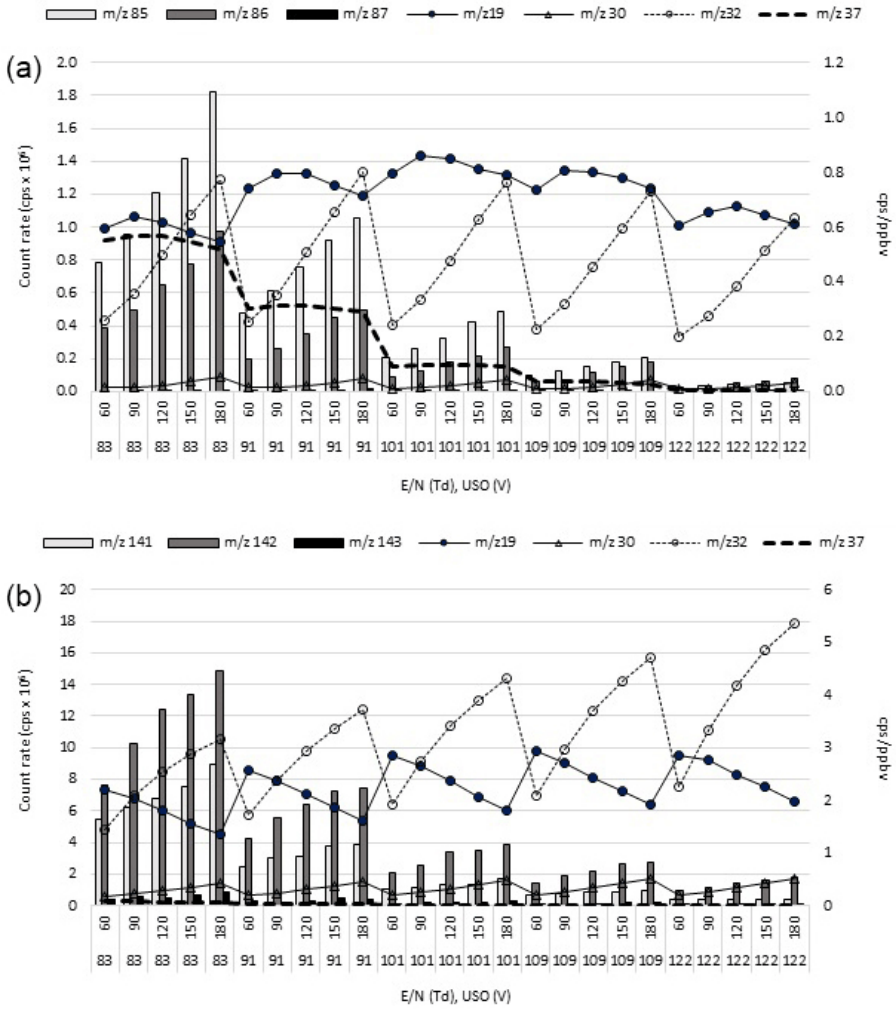

Figure 2. Intensity of signals (counts per second, cps) for H_3O^+ (m/z 19), NO^+ (m/z 30), O_2^+ (m/z 32), $H_2O \cdot (H_3O)^+$ (m/z 37) and sensitivities (cps ppbv^{-1}) at low water flow (2 sccm) for **(a)** n-hexane and **(b)** n-decane. Data are shown for tests at five E/N ratios (83, 91, 101, 109 and 122 Td) and five U_{SO} voltages (60, 90, 120, 150 and 180).

ted for n-hexane and for n-decane, produced from the HA, CT and PT mechanisms. The highest sensitivity for n-hexane was obtained by HA (m/z 85) followed by CT (m/z 86). PT (m/z 87) sensitivities were negligible (< 1 % with respect to HA). In the case of n-decane, maximum sensitivities were obtained by CT (m/z 142), followed by HA (m/z 141). Sensitivities by PT were < 8 % with respect to CT. n-Nonane, n-undecane and n-dodecane (Fig. S1) showed the same sensitivity trend as n-decane (Fig. 2b).

H_3O^+ and O_2^+ were the most abundant primary ions in all experiments. O_2^+ and NO^+ clearly increased with U_{SO} voltage, while water clusters decreased. Lower H_3O^+ abundance was used in the n-hexane experiments compared to the larger n-alkanes experiments because the water flow rate affected the absolute count rate of primary ions, and thus the water flow rate was changed. However, the reaction mechanisms are clearly demonstrated with hydride abstraction occurring for n-hexane and charge transfer for n-decane.

Table 2 shows the comparisons in sensitivities for the different mechanisms. We also compared these sensitivities under "typical" PTR-MS conditions to analyze VOCs: water flow 6 sccm, E/N ratio 122 Td and U_{SO} 60 V. Sensitivities for some ions in "typical" conditions were close to zero. However, under optimized conditions, sensitivities of n-hexane by HA were 344 times higher than sensitivities by PT and 1.9 times higher than by CT. In the case of higher n-alkanes, sensitivities by CT were higher than by PT but the ratios decreased consistently with the chain length, with higher PT for larger n-alkanes due to increasing proton affinities. A constant effect throughout the chain length was observed for the sensitivities ratios between CT and HA. Table 2 shows why, under typical PTR-MS conditions, n-alkanes are not detected by PT and emphasizes the novelty of

Table 2. Sensitivity ratios for different mechanisms: $[M^+]$ charge transfer, $[M-H]^+$ hydride abstraction and $[M+H]^+$ proton transfer. Dominant mechanism is shown in parenthesis.

n-Alkane	Optimized conditions 2 sccm, 83 Td, 180 V	Usual conditions 6 sccm, 122 Td, 60 V	Optimized conditions 2 sccm, 83 Td, 180 V	Usual conditions 6 sccm, 122 Td, 60 V
(HA)	$[M-H]^+/[M+H]^+$		$[M-H]^+/M^+$	
n-Hexane	344.0	$[M+H]^+$ = n.d.	1.9	M^+ = n.d.
(CT)	$M^+/[M+H]^+$		$M^+/[M-H]^+$	
n-Nonane	50.5	M^+, $[M+H]^+$ = n.d.	2.4	M^+, $[M-H]^+$ = n.d.
n-Decane	17.6	$[M+H]^+$ = n.d.	1.6	1.1
n-Undecane	8.0	$[M+H]^+$ = n.d.	1.6	0.5
n-Dodecane	3.5	$[M+H]^+$ = n.d.	1.6	1.0

n.d. – not detected.

the mixed mode. Under optimized conditions, our methodology can be used to detect n-alkanes not only from fossil sources but also from other sources, where their concentrations are extremely low and high sensitivity is needed. Maximum sensitivities were observed by CT and HA when water flow was significantly reduced (2 sccm in this study); thus further discussion will deal only with this low flow condition and will focus on O_2^+ and NO^+ ionizations.

3.2.1 O_2^+ and NO^+ ionizations

Molecules with IEs lower than the recombination energy of NO^+ (9.26 eV) may undergo charge transfer (Ellis and Mayhew, 2014; Lias, 2000), for example, aromatics and alkenes (Karl et al., 2012; Liu et al., 2013). n-Alkanes in this study have IEs (Table 1) higher than NO^+, so no charge transfer was expected. Therefore, charge transfer theoretically should be exclusively due to O_2^+. Figure 3a illustrates strong positive associations between O_2^+ and the signal of n-decane in CT (m/z 142, $r^2 \geq 0.97$). Similar behavior was observed for n-nonane, n-undecane and n-dodecane (Fig. S2). Reactions between O_2^+ and n-alkanes have been suggested to result from the CT mechanism (Arnold et al., 1997; Francis et al., 2007; Španěl and Smith, 1998; Wilson et al., 2003) at or close to the collisional rate (Lias et al., 1976; Searles and Sieck, 1970), except for methane (Barlow et al., 1986).

The relative abundance of the molecular ion reaction product increased with O_2^+ and decreased with E/N due to higher fragmentation (Fig. S3). Fragments m/z 57 $[C_4H_9]^+$, m/z 71 $[C_5H_{11}]^+$, m/z 85 $[C_6H_{13}]^+$, m/z 99 $[C_7H_{15}]^+$ and m/z 113 $[C_8H_{17}]^+$ were the most abundant at lower E/N ratios, but m/z 43 $[C_3H_7]^+$ and in particular m/z 29 $[C_2H_5]^+$ were the most abundant at higher E/N ratios. This was observed for all n-alkanes. CT in O_2^+ is dissociative and produces multiple product ions (Španěl and Smith, 1998). The identification of n-alkanes or other compounds in highly complex mixtures using the actual conditions is difficult and therefore has not yet been widely utilized. However, we comprehensively

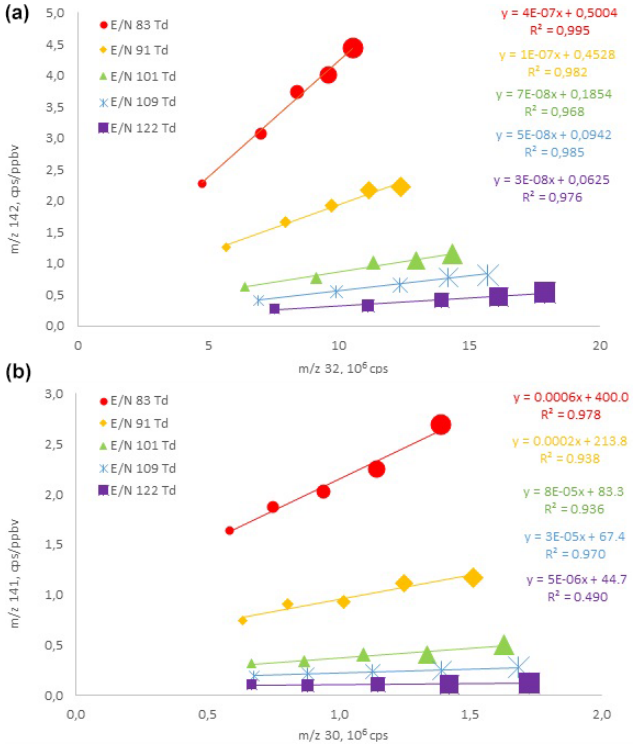

Figure 3. Intensities of **(a)** m/z 142 (M^+, charge transfer) vs. m/z 32 (O_2^+) for n-decane and **(b)** m/z 141 ($[M-H]^+$, hydride abstraction) vs. m/z 30 (NO^+) for n-decane. Marker size illustrates the U_{SO} values: smallest is 60 V and largest is 180 V.

approach these challenges and show that varying E/N ratio results in different proportions of these common fragments. The interferences and sensitivities are always a general issue for all ionization modes and in particular for quadrupole detectors and even more when fragmentation is high. While this can be an issue at trace levels of n-alkanes in biogenically influenced air (where isoprene oxidation products can result in the same nominal masses), this should not be a problem

for characterizing crude oil evaporation or alkane presence in pollution plumes dominated by n-alkanes. Potential interferences could be from alkenes but they are not present in the crude oil and their presence and abundance can also be inferred from different mechanisms.

O_2^+ has been reported to produce significant yields of HA species for ethane (55 %) and propane (40 %) (Francis et al., 2007), although Arnold et al. (1997) reported 2 % [$C_8H_7^+$] for n-octane. Unlike in the case of O_2^+, NO^+ has been shown to react by HA for $\geq C_5$ n-alkanes (Arnold et al., 1997, 1998; Španěl and Smith, 1998). This is illustrated in Fig. 3b where high correlations were obtained between products of HA and NO^+ ($r^2 = 0.94$–0.99, $E/N \leq 109$ Td). Because in our study NO^+ was mixed with O_2^+ (1 : 10) we cannot distinguish the dominant ion for HA using PTR-MS.

Enthalpy is one reason to explain the low sensitivities of $[M-H]^+$ species for smaller n-alkanes with NO^+. Formation of $[M-H]^+$ by reaction between NO^+ and n-alkanes ($\leq C_5$) has been reported to be endothermic (Hunt and Harvey, 1975; Arnold et al., 1998). In addition, the reaction rate constants decrease with carbon chain length for the n-alkanes (Arnold et al., 1998; Hunt and Harvey, 1975; Lias et al., 1976; Searles and Sieck, 1970; Španěl and Smith, 1998, Wilson et al., 2003). Arnold et al. (1998) observed 20 % yields for $[M-H]^+$ species in the reaction of n-hexane with H_3O^+, while < 5 % was observed in the reactions with n-heptane to n-decane. Similarly, Wilson et al. (2003) reported yields of 30 % of $[M-H]^+$ species on n-butane with H_3O^+. However, the rate constant reported by Arnold et al. (1998) was 0.006×10^{-9} cm^3 s^{-1}, while Wilson et al. (2003) did not report the rate constant. Španěl and Smith (1998) and Francis et al. (2007) did not report $[M-H]^+$ species from reaction between n-alkanes and H_3O^+. In our study we did not find any correlation between H_3O^+ signal with hydride abstraction species for any of the n-alkanes studied.

3.2.2 H_3O^+ effects

In our study, $[M+H]^+$ species were not observed for n-alkanes smaller than n-decane. For larger n-alkanes, a small signal intensity for $[M+H]^+$ was observed, which increased with increasing carbon chain length (Figs. 2, S1). The formation of $[M+H]^+$ species for short-chain n-alkanes is difficult because the reaction does not proceed at the collisional rate, but the proton transfer reaction of H_3O^+ with n-alkanes larger than n-hexane is expected to be exothermic (Arnold et al., 1998).

The $[M+H]^+$ did not correlate with H_3O^+, indicating it is not the proton donor, suggesting no significant direct proton transfer occurs between H_3O^+ and n-alkanes in this system. The same results were reported by Arnold et al. (1998), who observed no direct proton transfer product ions in the form $C_nH_{2n+3}^+$ ($N_c = 2$–12) in their SIFT experiments. Španěl and Smith (1998) also did not observe protonated parent alkanes ($N_c = 4$–12), apparently due to their instability in SIFT experiments. No direct proton transfer reaction is expected for formation of $[M+H]^+$ from n-alkanes by PT from water clusters (Jobson et al., 2005), because the proton affinities for these compounds are lower than the water cluster.

Instead of direct proton transfer to n-alkanes, $[M \cdot H_3O]^+$ species have been observed to be produced through an association mechanism between n-alkanes and H_3O^+ primary ion (Jobson et al., 2005; Španěl and Smith, 1998) (Reaction R6). Španěl and Smith (1998) observed in SIFT experiments that reaction of H_3O^+ with n-alkanes occurs near the collisional limit to form only association product ions as $[M \cdot H_3O]^+$. These species occur when the proton affinity is less than the proton affinity of water and proton transfer is endothermic (Smith and Španěl, 2005). We observed $[M \cdot H_3O]^+$ species formed from n-alkanes as illustrated by the adduct of n-decane at m/z 161 (Fig. S3). Positive correlations between hydronium and n-decane adduct [n–$C_{10}H_{22} \cdot H_3O]^+$ (m/z 161) with H_3O^+ (Fig. 4a) were observed. Similar correlations were found with $H_2O \cdot (H_3O)^+$ (Reaction R7). Higher H_3O^+ is produced at lower O_2^+ and, therefore, more $[M \cdot H_3O]^+$ was observed under these conditions. Similarly, a higher abundance of water clusters is produced at lower E/N ratio, and more $[M \cdot H_3O]^+$ was observed at lower O_2^+. Once the $[M \cdot H_3O]^+$ is formed, a collisional dissociation can take place producing $[M+H]^+$ (Reaction R8, Fig. 4b). An inverse relationship between $[C_{10}H_{22} \cdot H_3O]^+$ and $[M+H]^+$ (m/z 143) was observed. At higher O_2^+, more de-clustering occurs, decreasing $[M \cdot H_3O]^+$ and increasing $[M+H]^+$.

Therefore, we propose that $[M+H]^+$ comes from the adduct formation from $[M \cdot H_3O]^+$ found for these compounds (Reactions R6 and R7) and a subsequent collisional dissociation (Reaction R8).

$$H_3O^+ + n - C_{10}H_{22} \rightarrow [n - C_{10}H_{22} \cdot H_3O]^+$$
Adduct formation (R6)

$$H_2O \cdot (H_3O)^+ + n - C_{10}H_{22} \rightarrow [n - C_{10}H_{22} \cdot H_3O]^+ + H_2O$$
Ligand switching reaction (R7)

$$[n - C_{10}H_{22} \cdot H_3O]^+ + M \rightarrow [n - C_{10}H_{22} \cdot H]^+ + H_2O + M$$
Collisional dissociation (R8)

$$[n - C_{10}H_{22} \cdot H_3O]^+ + H_2O \rightarrow H_2O \cdot (H_3O)^+ + n - C_{10}H_{22}$$
Ligand switching (R9)

Španěl and Smith (1998) observed ligand switching between $[M \cdot H_3O]^+$ and the H_2O in SIFT experiments when a trace of water vapor was present in the carrier gas (Reaction R9). This can catalyze the production of the hydrated hydronium ion via Reactions R6 and R9. Switching reactions usually occur at the collisional rate, including reactions with alkanes (Španěl and Smith, 1998). Maximum $[M \cdot H_3O]^+ / M^+$ percentages were observed in higher E/N ratios and lower U_{SO}. The stability of these species is prob-

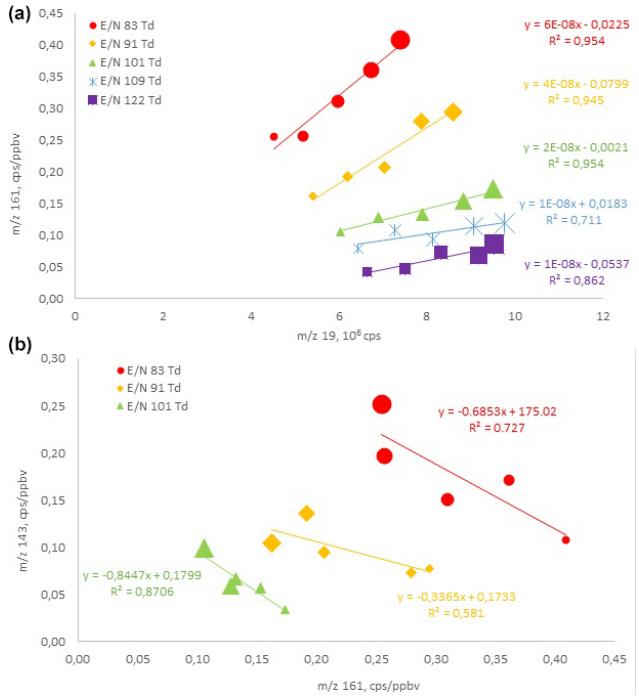

Figure 4. Intensities of the n-decane-water cluster (m/z 161, $M \cdot H_3O^+$) vs. **(a)** hydronium (m/z 19, H_3O^+) and **(b)** proton transfer product (m/z 143, $M + H^+$). Marker size illustrates the U_{SO}: smallest is 60 V and largest is180 V. No correlations were observed at 109 and 122 Td.

ably due to an ion-induced dipole interaction strengthened by the higher polarizability of larger alkanes (Anslyn and Dougherty, 2006), increasing the bond strength of the cluster (Arnold et al., 1998). The rates of such association reactions apparently increase as the proton affinity approaches that of water (Španěl and Smith, 1998).

3.3 Sensitivities and linearity of response

The optimal PTR-MS conditions were applied to determine the response linearity of the n-alkanes. Experiments were carried out at 83 Td, $U_{SO} = 180$ V and $H_3O^+ = 1$ sccm. We extended the number of n-alkanes from n-pentane to n-tridecane. Table S1 indicates the range of concentrations tested.

Since the sensitivity (cps ppbv^{-1}) of target compounds is a function of the primary ion abundance, and the absolute values of water flow in different PTR-MS instruments may result in different levels of O_2^+, normalized sensitivity (ncps ppbv^{-1}) is recommended to account for their variability (Jobson et al., 2005; Warneke et al., 2001). H_3O^+ is normally used when proton transfer is the dominant mechanism. However, in our study, we calculated four types of sensitivities: absolute, normalized to O_2^+, normalized to NO^+ and normalized to the sum of $O_2^+ + NO^+$, for all n-alkanes. To determine which approach is the best metric for sensitivity comparisons, we compared the sensitivities for n-nonane, n-decane, n-undecane and n-dodecane obtained in the first and the second set of experiments. These n-alkanes followed exactly the same mechanisms among them, as described earlier. Figure S4 shows stabilities of sensitivities. Normalized sensitivities to O_2^+ resulted in the minimum variability in sensitivities by HA reactions, while the normalization to the sum of $[O_2^+ + NO^+]$ resulted in the minimum variability in sensitivities by CT reactions. Results suggest that normalization to both ions makes sense for CT and that normalization to O_2^+ makes the most sense for HA.

Figure 5 shows the normalized and weighted to O_2^+ sensitivities for all nine n-alkanes determined in the optimized conditions. To be consistent with terms used by the PTR-MS community, we use "ncps" for the PT mechanism normalized to 1 million cps of H_3O^+ (Fig. 5a). The CT (Fig. 5b) and DHA (Fig. 5d) mechanisms in the case of n-alkanes are due to O_2^+ so we present "weighted" sensitivities wcps/ppbv (to distinguish from PTR terms) where signals are normalized to 1 million cps of O_2^+. In the case of HA mechanisms (Fig. 5c), which can undergo O_2^+ ionization, NO^+ ionization or both, we present "weighted" sensitivities wcps/ppbv which are normalized to 1 million cps of the sum of NO^+ and O_2^+. As we observed previously in the first set of experiments, CT was the dominant mechanism for n-heptane and larger n-alkanes, while HA was dominant for n-hexane and n-pentane. The limits of detection (LODs) are dependent on the sensitivity and standard deviation of the VOC-free background (dependent on the amount of averaging and other factors). LODs depend on the averaging times, ionization mechanism and instrument-dependent background. LODs for n-alkanes studied here are calculated to be between 10 ppt for n-dodecane and 460 ppt for n-hexane, with averaging times of 0.2 s. These LODs are at the lower end of what is useful in the ambient atmosphere under relatively unpolluted conditions, but they seem promising for studies in polluted environments or in regions where oil evaporation is occurring. Furthermore, longer averaging times can be used to reduce the detection limit further.

3.3.1 Dependence of CT sensitivity on ionization energy

The sensitivities to reaction by charge transfer for the n-alkanes was observed to be proportional to the chain length from n-pentane to n-dodecane (Fig. 5b). This is due to the higher polarizability and stability of larger n-alkanes (Cao and Yuan, 2002), as shown by the exponentially negative association between their normalized sensitivities and IEs (Fig. 6) ($wSens = 5E + 43x^{-42.23}$, $r^2 = 0.98$, $n = 9$). The sensitivities to reaction by HA also increased with the chain length from n-heptane, but sensitivities to n-pentane and n-hexane were higher than n-heptane (Fig. 5c). PT reactions increased sensitivities from n-decane in our study (Fig. 5a). However, negligible or no PT products were found in this study for n-alkanes smaller than n-decane. Meanwhile a de-

Table 3. Fragment contribution distribution (FCD, %) from larger n-alkanes to smaller n-alkanes.

	Smaller n-alkane	n-Pentane	n-Hexane	n-Heptane	n-Octane	n-Nonane	n-Decane	n-Undecane	n-Dodecane
Larger n-alkane	m/z	72	86	100	114	128	142	156	170
n-Hexane	86	96.7							
n-Heptane	100	153.9	8.6						
n-Octane	114	59.0	138.1	0.7					
n-Nonane	128	31.0	61.2	12.9	0.0				
n-Decane	142	28.7	34.4	8.6	8.8	0.2			
n-Undecane	156	21.0	18.5	5.2	6.3	5.6	0.5		
n-Dodecane	170	15.1	11.5	2.8	4.5	5.0	5.3	0.6	
n-Tridecane	184	11.5	8.4	1.9	3.0	4.3	5.9	6.6	1.0

crease in sensitivity to reaction by CT and HA was observed for n-tridecane, an increase in the PT sensitivity was observed when the carbon number increased. This trend was previously shown by SIFT studies for larger n-alkanes by the PT mechanism, where the reactions with H_3O^+ become more exothermic (Arnold et al., 1998).

3.3.2 Double hydride abstraction

Figures 5d and 7 demonstrate the observation of DHA products from n-alkanes. DHA/CT products shown in Fig. 7 provide a better visualization of the abundance for n-pentane and n-hexane. Little information has been reported on DHA mechanisms. Francis et al. (2007) reported DHA yields from ethane (15 %) and propane (5 %) in the presence of O_2^+, while dissociation was reported for higher n-alkanes ($N_c = 4$–9). Arnold et al. (1997) reported DHA in the reaction of n-octane (1 %) and isooctane (7 %) with O_2^+. Positive correlations of DHA for n-hexane and n-decane vs. O_2^+ (Fig. S5) were obtained, suggesting DHA is driven by O_2^+.

3.4 Example application of the calibrated fragment algorithm for quantifying n-alkanes mixtures

Fragmentation of n-alkanes under O_2^+ mode (Fig. S3) creates a challenge for quantifying individual n-alkanes in mixtures. We applied the algorithm introduced in Sect. 2.3 to calculate n-decane (m/z 142) concentration (taken as an example) measured in a test mixture including nine n-alkanes. Details of the calculation are shown in the Supplement.

Table 3 presents the fragment contributions from larger n-alkanes to smaller n-alkanes. Less than 15 % contribution to the signal was observed from fragments of n-alkanes larger than n-hexane. Fragment contributions on m/z 72 (n-pentane) and m/z 86 (n-hexane) were observed to increase with larger n-alkane length. However, the algorithm successfully subtracted fragments of larger alkanes from the lower alkane signals, demonstrating that this method works reasonably well and is easy to apply. Table 4 shows the standard n-alkane concentration in the mixture compared to the measured n-alkane concentration determined using the algorithm, and the bias. This experiment was done at three different concentration levels. The largest bias (around 30 %) was observed for n-octane and n-tridecane. The bias for the rest of n-alkanes was lower than 20 %. n-Pentane experiments showed injection problems due to fast evaporation of n-pentane in the syringe pump during injection into the flow tube, so it was only possible to determine the concentration at one concentration level.

3.5 Measuring n-alkanes in the gas phase of evaporated oil

The algorithm was also evaluated by quantifying n-alkanes in a real world very complex example. A sample of MC252 oil (see the Supplement for more details) was evaporated in a wind tunnel. The gas phase evaporation was monitored by the PTR-MS operating in optimized mixed ionization mode conditions and the remaining liquid oil was monitored by GC × GC. Figure 8 shows a summary of the evaporated n-alkanes integrated over the sampling period, the initial concentrations of n-alkanes in the liquid phase oil (analyzed using GC × GC) and the sum of evaporated alkanes plus alkanes remaining in the oil after 2, 8 and 12 h. Using GC × GC analysis we determined the initial and final n-alkane amounts in the oil and found it agreed well with the evaporated amount measured with the PTR-MS analysis, within −2 % for n-decane, −10 % for n-undecane, +4 % for n-dodecane and +2 % for n-tridecane. The agreement of evaporated plus remaining n-alkanes compared to the initial oil concentrations demonstrates quantitative agreement between the PTR-MS and GC × GC techniques and that n-alkane evaporation is a function of vapor pressure and number of C in the molecule. The two-dimensional chromatogram of fresh oil MC252 is shown in Fig. S6.

Our methodology is an option to detect/quantify n-alkanes in complex mixtures. However, our methodology should be further tested in different complex mixtures to demonstrate

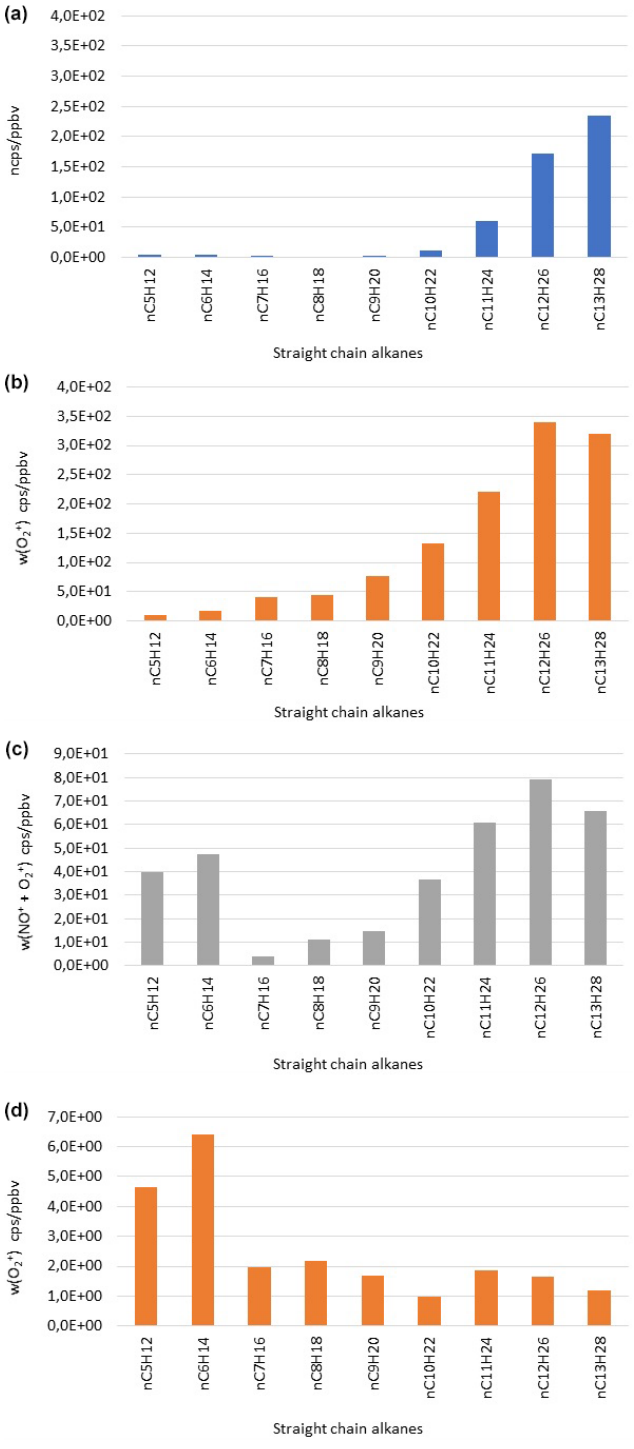

Figure 5. Sensitivities for straight chain alkanes detected by different mechanisms: **(a)** proton transfer, normalized to H_3O^+; **(b)** charge transfer, weighted to sum ($NO^+ + O_2^+$); **(c)** hydride abstraction, weighted to sum ($NO^+ + O_2^+$); **(d)** double hydride abstraction, weighted to O_2^+.

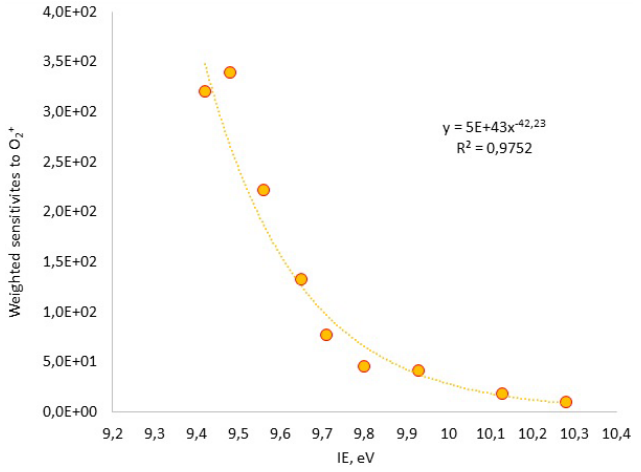

Figure 6. Ionization energy vs. sensitivities weighted to O_2^+ for n-alkanes reacting via charge transfer.

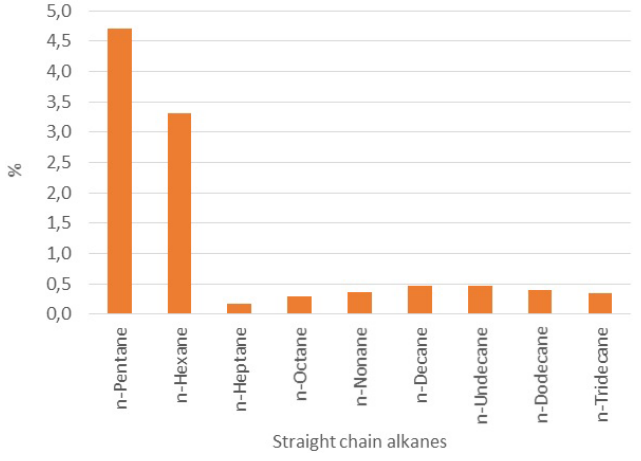

Figure 7. Contribution of double hydride abstraction (DHA) to charge transfer (CT), calculated using weighted sensitivities [$w(O_2^+)$ cps ppbv^{-1}] normalized to O_2^+.

its performance, as this is the most challenging application for detection of n-alkanes.

4 Conclusions

We explored and optimized mixed ionization mode conditions in the PTR-MS to enhance the detection of n-alkanes. Ionization using a combination of O_2^+ and NO^+, along with H_3O^+, allowed access to multiple ionization mechanisms with different sensitivities and specificities for n-alkanes. Low water flow (2 sccm), low E/N ratio (83 Td) and high O_2^+ ($U_{so} = 180$ V) provided the best overall conditions for analysis of n-alkanes. The charge transfer mechanism produced the maximum sensitivities for n-alkanes higher than n-hexane, followed by the hydride abstraction mechanism. Hydride abstraction was the most sensitive mechanism for n-

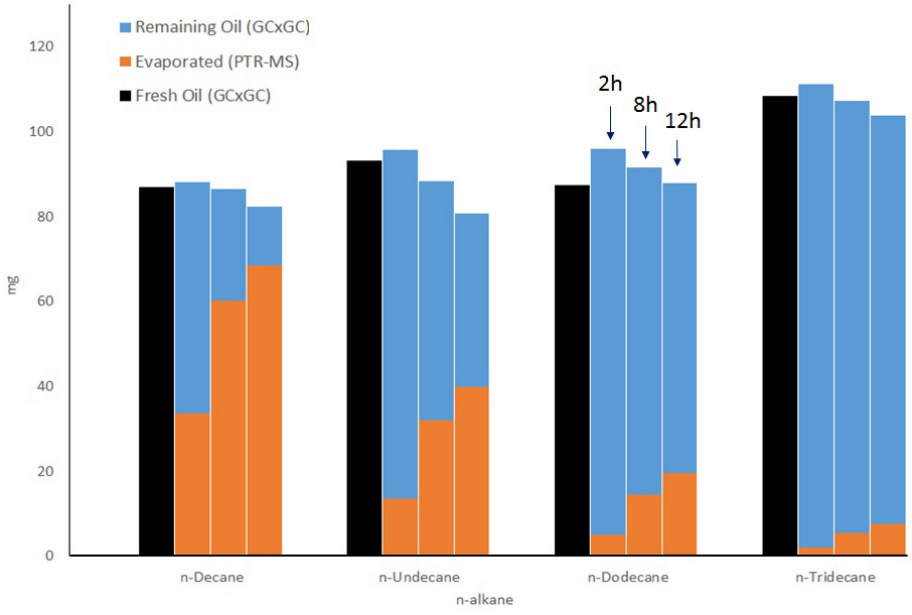

Figure 8. *n*-Alkane mass in fresh oil as measured by GC × GC and *n*-alkanes at different evaporation times (2, 8 and 12 h) as measured by PTR-MS (gas phase) and remaining in the oil as measured using GC × GC (liquid phase). The sum of evaporated and remaining *n*-decane, *n*-undecane, *n*-dodecane and *n*-tridecane is in good agreement with the amount in the fresh oil. Alkanes more volatile than *n*-decane were not observed quantitatively by the GC × GC analysis.

Table 4. Potential bias of *n*-alkanes concentrations estimated with the algorithm vs. experimental concentrations indicated in Table S2. Bias (%) at three concentration levels. *n*-alkanes in the mixture.

n-Alkane	Experimental ppbv	Algorithm ppbv	Bias %	Experimental ppbv	Algorithm ppbv	Bias %	Experimental ppbv	Algorithm ppbv	Bias %
n-Pentane	106.3	112.5	5.9	247.8	n.e.	n.e.	394.7	n.e.	n.e.
n-Hexane	89.0	81.5	−8.4	218.7	175.3	−19.8	277.6	262.7	−5.4
n-Heptane	79.3	92.7	16.9	194.9	205.3	5.3	247.4	273.7	10.6
n-Octane	71.5	96.7	35.2	175.7	222.2	26.4	223.1	292.0	30.9
n-Nonane	65.0	71.1	9.3	159.8	181.8	13.7	202.9	211.3	4.1
n-Decane	60.0	57.0	−5.0	147.5	140.1	−5.0	187.2	166.8	−10.9
n-Undecane	55.0	51.9	−5.5	135.2	129.9	−3.9	171.6	162.0	−5.6
n-Dodecane	51.1	51.1	0.1	125.6	116.0	−7.6	159.4	152.8	−4.1
n-Tridecane	47.6	63.0	32.5	116.9	151.9	29.9	148.4	198.6	33.8

n.e. – not estimated due to experimental problems.

hexane and *n*-pentane, followed by charge transfer and double hydride extraction. Sensitivities to charge transfer and hydride abstraction increased with carbon chain length from *n*-pentane to *n*-dodecane for CT and from *n*-heptane to *n*-dodecane for HA. Proton transfer was not observed for *n*-alkanes with carbon chain lengths from five to nine. From *n*-decane, the sensitivity to proton transfer increased with carbon chain length. Ionization by O_2^+ was sensitive through both charge transfer and double hydride abstraction, while with NO^+ only hydride abstraction was observed. No direct proton transfer was observed for *n*-alkanes but relatively small water cluster $[M \cdot H_3O]^+$ formation was observed with a tendency to dissociate to $[M + H]^+$ species. We observed an exponentially negative association between the normalized sensitivities under charge transfer and molecular ionization energies due to polarizability and stability of the larger *n*-alkanes. The identification of a double hydride abstraction mechanism by O_2^+ ionization is a new insight providing a novel selective and sensitive detection approach for measuring *n*-pentane and *n*-hexane with PTR-MS. We developed an algorithm to quantify the signal attributable to individual *n*-alkanes in complex mixtures by subtracting the fragments due to larger alkanes. This method works reasonably well for mixtures of *n*-alkanes and is easy to apply. The conditions determined in this study allow for the use of PTR-MS to sensitively measure *n*-alkanes in mixed ionization mode.

This approach could also be extended to other alkane compounds like branched and cycloalkanes that constitute important mass fractions of petroleum-derived products which are not measured with traditional PTR-MS. Our comprehensive study of the ionization schemes allows us to determine the major components of a sample and may often allow much more detailed characterization than has previously been possible.

5 Data availability

Data for this study have been included in tables and figures of the main paper and Supplement. Specific data requests can be directed to oam@atmosfera.unam.mx.

The Supplement related to this article is available online at doi:10.5194/amt-9-5315-2016-supplement.

Acknowledgements. AMO acknowledges financial support of UCMEXUS-CONACyT Program for the Postdoctoral Fellowship. This research was made possible by a grant from the Gulf of Mexico Research Initiative (GOMRI), as part of the Gulf of Mexico Integrated Spill Response Consortium (GISR) under contract SA12-09/GoMRI-006. Authors thank Nathan M. Kreisberg for use of the wind tunnel.

Edited by: J. Curtius
Reviewed by: two anonymous referees

References

Amador-Muñoz, O., Villalobos-Pietrini, R., Miranda, J., and Vera-Avila, L. E.: Organic compounds of $PM_{2.5}$ in Mexico Valley: Spatial and temporal patterns, behavior and sources, Sci. Total Environ., 409, 1453–1465, doi:10.1016/j.scitotenv.2010.11.026, 2011.

Anslyn, E. V. and Dougherty, D. A.: Modern physical organic chemistry, University Science Book, USA, 1111 pp., 2006.

Arnold, S. T., Viggiano, A. A., and Morris, R. A.: Rate Constants and Branching Ratios for the Reactions of Selected Atmospheric Primary Cations with n-Octane and Isooctane (2,2,4-Trimethylpentane), J. Phys. Chem. A, 101, 9351–9358, doi:10.1021/jp972106v, 1997.

Arnold, S. T., Viggiano, A. A., and Morris, R. A.: Rate constants and product branching fractions for the reactions of H_3O^+ and NO^+ with C2–C12 alkanes, J. Phys. Chem. A, 102, 8881–8887, doi:10.1021/jp9815457, 1998.

Barlow, S. E., Van Doren, J. M., DePuy, C. H., Bierbaum, V. M., Dotan, I., Ferguson, E. E., Adams, N. G., Smith, D., Rowe, B. R., Marquette, J. B., Dupeyrat, G., and Durup-Ferguson, M.: Studies of the reaction of O_2^+ with deuterated methanes, J. Chem. Phys., 85, 3851–3859, doi:10.1063/1.450905, 1986.

Blake, R. S., Wyche, K. P., Ellis, A. M., and Monks, P. S.: Chemical ionization reaction time-of-flight mass spectrometry: multi-reagent analysis for determination of trace gas composition, Int. J. Mass Spectrom., 254, 85–93, doi:10.1016/j.ijms.2006.05.021, 2006.

Cao, C. and Yuan, H.: On Molecular Polarizability. 4. Evaluation of the Ionization Potential for Alkanes and Alkenes with Polarizability, J. Chem. Inf. Comput. Sci., 42, 667–672, doi:10.1021/ci010344o, 2002.

de Gouw, J. and Warneke, C.: Measurements of volatile organic compounds in the earth's atmosphere using proton-transfer mass spectrometry, Mass Spectrom. Rev., 26, 223–257, doi:10.1002/mas.20119, 2007.

de Gouw, J., Warneke, C., Karl T., Eerdekens, G., van der Veen, C., and Fall, R.: Sensitivity and specificity of atmospheric trace gas detection by proton-transfer-reaction mass spectrometry, Int. J. Mass Spectrom., 223–224, 365–382, doi:10.1016/S1387-3806(02)00926-0, 2003.

Drozd, G. T., Worton, D. R., Aeppli, C., Reddy, C. M., Zhang, H., Variano, E., and Goldstein, A. H.: Modeling comprehensive chemical composition of weathered oil following a marine spill to predict ozone and potential secondary aerosol formation and constrain transport pathways, J. Geophys. Res.-Oceans, 120, 7300–7315, doi:10.1002/2015JC011093, 2015.

Ellis, A. M. and Mayhew, C. A.: Proton transfer reaction mass spectrometry, Principles and applications, John Wiley & Sons Ltd., UK, 350 pp., 2014.

Erickson, M. H., Gueneron, M., and Jobson, B. T.: Measuring long chain alkanes in diesel engine exhaust by thermal desorption PTR-MS, Atmos. Meas. Tech., 7, 225–239, doi:10.5194/amt-7-225-2014, 2014.

Francis, G. J., Wilson, P. F., Milligan, D. B., Langford, V. S., and McEwan, M. J.: GeoVOC: A SIFT-MS method for the analysis of small linear hydrocarbons of relevance to oil exploration, Int. J. Mass Spectrom., 268, 38–46, doi:10.1016/j.ijms.2007.08.005, 2007.

Gentner, D. R., Isaacman, G., Worton, D. R., Chan, A. W. H., Dallmann, T. R., Davis, L., Liu, S., Day, D. A., Russell, L. M., Wilson, K. R., Weber, R., Guha, A., Harley, R. A., and Goldstein, A. H.: Elucidating secondary organic aerosol from diesel and gasoline vehicles through detailed characterization of organic carbon emissions, P. Natl. Acad. Sci. USA, 109, 18318–18323, doi:10.1073/pnas.1212272109, 2012.

Gentner, D. R., Worton, D. R., Isaacman, G., Davis, L. C., Dallmann, T. R., Wood, E. C., Herndon, S. C., Goldstein, A. H., and Harley, R. A.: Chemical Composition of Gas-Phase Organic Carbon Emissions from Motor Vehicles and Implications for Ozone Production, Environ. Sci. Technol., 47, 11837–11848, doi:10.1021/es401470e, 2013.

Hansel, A., Jordan, A., Holzinger, R., Prazeller, P., Vogel, W., and Lindinger, W.: Proton transfer reaction mass spectrometry: on-line trace gas analysis at the ppb level, Int. J. Mass Spectrom. Ion Proc., 149–150, 609–619, 1995.

Holzinger, R., Lee, A., Paw, K. T., and Goldstein, U. A. H.: Observations of oxidation products above a forest imply biogenic emissions of very reactive compounds, Atmos. Chem. Phys., 5, 67–75, doi:10.5194/acp-5-67-2005, 2005.

Hunt, D. F. and Harvey, M.: Nitric Oxide Chemical Ionization Mass Spectra of Alkanes, Anal Chem., 47, 1965–1969, doi:10.1021/ac60362a030, 1975.

Hunter, K. C. and East, A. L. L.: Properties of C-C Bonds in n-Alkanes: Relevance to Cracking Mechanisms, J. Phys. Chem. A, 106, 1346–1356, doi:10.1021/jp0129030, 2002.

Hunter, E. P. and Lias, S. G.: Evaluated Gas Phase Basicities and Proton Affinities of Molecules: An Update, J. Phys. Chem. Ref. Data, 27, 413–656, doi:10.1063/1.556018, 1998.

Inomata, S., Tanimoto, H., and Yamada, H.: Mass spectrometric detection of alkanes using NO^+ chemical ionization in proton-transfer-reaction plus switchable reagent ion mass spectrometry, Chem. Lett., 43, 538–540, doi:10.1246/cl.131105, 2013.

Isaacman, G., Wilson, K. R., Chan, A. W. H., Worton, D. R., Kimmel, J. R., Nah, T., Hohaus, T., Gonin, M., Kroll, J. H., Worsnop, D. R., and Goldstein, A. H.: Improved Resolution of Hydrocarbon Structures and Constitutional Isomers in Complex Mixtures Using Gas Chromatography-Vacuum Ultraviolet-Mass Spectrometry, Anal. Chem., 84, 2335–2342, doi:10.1021/ac2030464, 2012.

Jobson, B. T., Alexander, M. L., Maupin, G. D., and Muntean, G. G.: On-line analysis of organic compounds in diesel exhaust using a proton transfer reaction mass spectrometer (PTR-MS), Int. J. Mass Spectrom., 245, 78–89, doi:10.1016/j.ijms.2005.05.009, 2005.

Jordan, A., Haidacher, S., Hanel, G., Hartungen, E., Herbig, J., Märk, L., Schottkowsky, R., Seehauser, H., Sulzer, P., and Märk, T. D.: An online ultra-high sensitivity Proton-transfer-reaction mass-spectrometer combined with switchable reagent ion capability ($PTR + SRI - MS$), Int. J. Mass Spectrom., 286, 32–38, doi:10.1016/j.ijms.2009.06.006, 2009.

Jordan, C. E., Ziemann, P. J., Griffin, R. J., Lim, Y. B., Atkinson, R., and Arey, J.: Modeling SOA formation from OH reactions with C_8–C_{17} n-alkanes, Atmos. Environ., 42, 8015–8026, doi:10.1016/j.atmosenv.2008.06.017, 2008.

Karl, T. G., Spirig, C., Rinne, J., Stroud, C., Prevost, P., Greenberg, J., Fall, R., and Guenther, A.: Virtual disjunct eddy covariance measurements of organic compound fluxes from a subalpine forest using proton transfer reaction mass spectrometry, Atmos. Chem. Phys., 2, 279–291, doi:10.5194/acp-2-279-2002, 2002.

Karl, T., Hansel, A., Cappellin, L., Kaser, L., Herdlinger-Blatt, I., and Jud, W.: Selective measurements of isoprene and 2-methyl-3-buten-2-ol based on NO^+ ionization mass spectrometry, Atmos. Chem. Phys., 12, 11877–11884, doi:10.5194/acp-12-11877-2012, 2012.

King, J., Mochalski, P., Kupferthaler, A., Unterkofler, K., Koc, H., Filipiak, W., Teschl, S., Hinterhuber, H., and Amann, A.: Dynamic profiles of volatile organic compounds in exhaled breath as determined by a coupled PTR-MS/GC-MS study, Physiol. Meas., 31, 1169–1184, 2010.

Knighton, W. B., Fortner, E. C., Herndon, S. C., Wood, E. C., and Miake-Lye, R. C.: Adaptation of a proton transfer reaction mass spectrometer instrument to employ NO^+ as reagent ion for the detection of 1,3-butadiene in the ambient atmosphere, Rapid Commun. Mass Spec., 23, 3301–3308, doi:10.1002/rcm.4249, 2009.

Koss, A. R., Warneke, C., Yuan, B., Coggon, M. M., Veres, P. R., and de Gouw, J. A.: Evaluation of NO+ reagent ion chemistry for online measurements of atmospheric volatile organic compounds, Atmos. Meas. Tech., 9, 2909-2925, doi:10.5194/amt-9-2909-2016, 2016.

Lias, S. G.: Ionization energy evaluation, in: NIST Chemistry WebBook, edited by: Mallard, W. G. and Linstrom, P. J., NIST Standard Reference Database Number 69, February, National Institute of Standards and Technology, Gaithersburg, MD, 2000.

Lias, S. G., Eyler, J. R., and Ausloos, P.: Hydride transfer reactions involving saturated hydrocarbons and CCl_3^+, CCl_2H^+, CCl_2F^+, CF_2Cl^+, CF_2H^+, CF_3^+, NO^+, $C_2H_5^+$, sec-$C_3H_7^+$ and t-$C_4H_9^+$, Int. J. Mass Spectrom. Ion Phys., 19, 219–239, 1976.

Lias, S. G., Liebman, J. F., and Levin, R. D.: Evaluated Gas Phase Basicities and Proton Affinities of Molecules; Heats of formation of Protonated Molecules, J. Phys. Chem. Ref. Data, 13, 695–808, doi:10.1063/1.555719, 1984.

Lim, Y. B. and Ziemann, P. J.: Products and Mechanism of Secondary Organic Aerosol Formation from Reactions of n-Alkanes with OH radicals in the Presence of NO_x, Environ. Sci. Technol., 39, 9229–9236, doi:10.1021/es051447g, 2005.

Lindinger, W., Hansel, A., and Jordan, A.: Proton-transfer-reaction mass spectrometry (PTR–MS): on-line monitoring of volatile organic compounds at pptv levels, Chem. Soc. Rev., 27, 347–354, 1998.

Linstrom, P. J. and Mallard, W. G. (Eds.): NIST Chemistry Web Book, NIST Standard Reference Database Number 69, National Institute of Standards and Technology, Gaithersburg MD, 20899, available at: http://webbook.nist.gov, June 2005.

Liu, Y. J., Herdlinger-Blatt, I., McKinney, K. A., and Martin, S. T.: Production of methyl vinyl ketone and methacrolein via the hydroperoxyl pathway of isoprene oxidation, Atmos. Chem. Phys., 13, 5715–5730, doi:10.5194/acp-13-5715-2013, 2013.

Searles, S. K. and Sieck, L. W.: High pressure photoionization Mass Spectrometry: III Reactions of $NO^+(X1\Sigma+)$ with C_3–C_7 Hydrocarbons at Thermal Kinetic Energies, J. Chem. Phys., 53, 794–798, doi:10.1063/1.1674061, 1970.

Smith, D. and Španěl P.: Selected Ion Flow Tube Mass Spectrometry (SIFT-MS) for On-line Trace Gas Analysis, Mass Spectrom. Rev., 24, 661–700, 2005.

Španěl, P. and Smith, D.: Selected ion flow tube studies of the reactions of H_3O^+, NO^+, and O_2^+ with several aromatic and aliphatic hydrocarbons, Int. J. Mass Spectrom., 181, 1–10, doi:10.1016/S1387-3806(98)14114-3, 1998.

Warneke, C., van der Veen, C., Luxembourg, S., de Gouw, J. A., and Kok, A.: Measurements of benzene and toluene in ambient air using proton-transfer-reaction mass spectrometry: calibration, humidity dependence, and field intercomparison, Int. J. Mass Spectrom., 207, 167–182, doi:10.1016/S1387-3806(01)00366-9, 2001.

Wilson, P. F., Freeman, C. G., and McEwan, M. J.: Reactions of small hydrocarbons with H_3O^+, O_2^+ and NO^+ ions, Int. J. Mass Spectrom., 229, 143–149, doi:10.1016/S1387-3806(03)00290-2, 2003.

Worton, D. R., Isaacman, G., Gentner, D. R., Dallmann, T. R., Chan, A. H. W., Ruehl, C. R., Kirchstetter, T. W., Wilson, K. R., Harley R. A., and Goldstein, A. H.: Lubricating Oil Dominates Primary Organic Aerosol Emissions from Motor Vehicles, Environ. Sci. Technol., 48, 3698–3706, doi:10.1021/es405375j, 2014.

Worton, D. R., Zhang, H., Isaacman-VanWertz, G., Chan, A. W. H., Wilson, K. R., and Goldstein, A. H.: Comprehensive Chemical Characterization of Hydrocarbons in NIST Standard Reference

Material 2779 Gulf of Mexico Crude Oil, Environ. Sci. Technol., 49, 13130–13138, doi:10.1021/acs.est.5b03472, 2015.

Wyche, K. P., Blake, R. S., Willis, K. A., Monks, P. S., and Ellis, A. M.: Differentiation of isobaric compounds using chemical ionization reaction mass spectrometry, Rapid Commun. Mass Spectrom., 19, 3356–3362, doi:10.1002/rcm.2202, 2005.

Zhang, H., Ruehl, C. R., Chan, A. W. H., Nah, T., Worton, D. R., Isaacman, G., Goldstein, A. H., and Wilson, K.: OH-Initiated Heterogeneous Oxidation of Cholestane: A Model System for Understanding the Photochemical Aging of Cyclic Alkane Aerosols, J. Phys. Chem. A, 117, 12449–12458, doi:10.1021/jp407994m, 2013.

Zhou, Z., Zhang, L., Xie, M., Wang, Z., Chen, D., and Qi, F.: Determination of absolute photoionization cross-sections of alkanes and cyclo-alkanes, Rapid Comm. Mass Spectrom., 24, 1335–1342, doi:10.1002/rcm.4523, 2010.